Protein Crystals as Novel Microporous Materials

Lev Z. Vilenchik, James P. Griffith,[†] Nancy St. Clair, Manuel A. Navia,[†,‡] and Alexey L. Margolin*

Contribution from Altus Biologics Inc., 40 Allston Street, Cambridge, Massachusetts 02139

Received October 2, 1997

Abstract: Cross-linked protein crystals (CLPCs) constitute a novel type of molecular sieves with high porosity. In order to characterize the fully hydrated CLPC, the method of macromolecular porosimetry was applied. This technique allows one to estimate the apparent pore sizes and pore size distribution in solid and soft hydrated porous sorbents directly from size exclusion chromatography. According to this method, CLPCs offer a wide range of pore size (15−100 Å), porosity (0.5−0.8), and pore surface area (800−2000 m^2/g). These CLPC materials can be made chemically and mechanically stable, and are capable of separating molecules by size, chemical structure, and chirality.

Introduction

Crystalline inorganic materials (zeolites and pillared layered solids) are widely used in catalysis and in separation applications.[1] The field of microporous organic solids, however, has only recently emerged.[2] A major challenge in the rational design of highly porous organic materials (organic zeolites) is their fragility.[3] Unlike zeolites which are bound together by strong covalent bonds, organic solid molecules are linked via much weaker noncovalent forces. As such, nanoscale cavities will tend to collapse in the course of the host−guest exchange.[4]

Here, we present evidence that useful microporous materials can be obtained by using protein crystals. The solvent content of typical protein crystals is comprised of uniform solvent-filled channels that ranges from 30% to 65% of the total crystal volume.[5] These channels traverse the body of a crystal and facilitate the transport of substrates and products in and out of the crystal (Figure 1). A distinct advantage of protein crystals over other porous materials is the inherently chiral nature of protein molecules. The L-amino acids that make up proteins create an asymmetric environment that can be exploited in the separation of enantiomers and in catalysis. Further, one can modify the microenvironment of these crystal channels (with respect to both charge and hydrophobicity) by well-known techniques of protein chemistry, or by crystallization of modified recombinant proteins expressly designed for this purpose.

Macromolecular crystals are held together by weak intermolecular interactions, and like their organic counterparts, they are soft and can easily disintegrate in unfavorable environments. As such, the properties of protein crystals as materials have not been explored, in spite of early indications that the mechanical stability of protein crystals could be enhanced through chemical cross-linking.[6] In recent studies we have demonstrated that cross-linked enzyme crystals (CLECs),[7] or more broadly cross-linked protein crystals (CLPCs), are stable against mechanical disruption and shear under mixing, filtration, and pumping[8] and can be economically produced on a large scale.[9] In addition, CLEC catalysts have been shown to be remarkably stable[10] and active[11] at elevated temperature and in aqueous, organic, and mixed solvents. These collective properties[12] have allowed CLECs to be successfully used as catalysts for peptide synthesis,[13,14] catalytic chiral resolutions,[15] and carbon−carbon bond formation.[16] The inherent porosity of protein crystals, combined with their unique stability in their CLEC or CLPC form, suggested that these materials might also prove useful as a novel class of molecular sieves which we designate as bioorganic zeolites.

Results and Discussion

Several analytical methods have been used to investigate the characteristics of porous materials. These methods include mercury intrusion porosimetry (MIP),[17] where elemental mer-

* Corresponding author. Phone: (617) 499 0500. Fax: (617) 499 2480. E-mail: margolin@altus.com.

[†] Vertex Pharmaceuticals Inc., 130 Waverly St., Cambridge, MA 02139.

[‡] Present address: The Althexis Co., P.O. Box 660, Bedford, MA 01730.

(1) . Arends, I. W. C. E.; Sheldon, R. A.; Wallau, M.; Schuhardt, U. *Angew. Chem., Int. Ed. Engl.* **1997**, *36*, 1144−1163.

(2) Service, R. F. *Science* **1994**, *265*, 1363. Moore, J. S. *Nature* **1995**, *374*, 495−496. Gardner, G. B.; Venkataraman, D.; Moore, J. S.; Lee, S. *Nature* **1995**, *374*, 792−795. Wang, X.; Simard, M.; Wuest, J. D. *J. Am. Chem. Soc.* **1994**, *116*, 12119−12120. Ward, M. *Nature* **1995**, *374*, 764−765.

(3) Venkataraman, D.; Lee, S.; Zhang, J.; Moore, J. S. *Nature* **1994**, *371*, 591−593.

(4) Abrahams, B. F.; Hoskins, B. F.; Michail, D. M.; Robson, R. *Nature* **1994**, *369*, 727−729.

(5) Matthews, B. W. *J. Mol. Biol.* **1968**, *33*, 491−497.

(6) Quiocho, F. A.; Richards, F. M. *Proc. Natl. Acad. Sci. U.S.A.* **1964**, *52*, 833−839.

(7) St. Clair, N. L.; Navia, M. A. *J. Am. Chem. Soc.* **1992**, *114*, 7314−7316.

(8) Lalonde, J. J.; Govardhan, C.; Persichetti, R. A.; Wang, Y. F.; Margolin, A. L. Proceedings of the InBio 96 Conference, Manchester, February 1996.

(9) Margolin, A. L. *Trends Biotechnol.* **1996**, *14*, 223−230.

(10) Govardhan, C.; Margolin, A. L. *Chem. Ind.* **1995**, 689−693.

(11) Khalaf, N.; Govardhan, C. P.; Lalonde, J. J.; Persichetti, R. A.; Wang, Y. F.; Margolin, A. L. *J. Am. Chem. Soc.* **1996**, *118*, 5494−5495.

(12) Zelinski, T.; Waldmann, H. *Angew. Chem., Int. Ed. Engl.* **1997**, *36*, 722−724.

(13) Persichetti, R. A.; St. Clair, N. L.; Griffith, J. P.; Navia, M. A.; Margolin, A. L. *J. Am. Chem. Soc.* **1995**, *117*, 2732−2737.

(14) Wang, Y.-F.; Yakovlevsky, K.; Margolin, A. L. *Tetrahedron Lett.* **1996**, *37*, 5317−5320.

(15) Lalonde, J. J.; Govardhan, C. P.; Khalaf, N. K.; Martinez, O. G.; Visuri, K. J.; Margolin, A. M. *J. Am. Chem. Soc.* **1995**, *117*, 6845−6852.

(16) Sobolov, S. B.; Bartoszko-Malik, A.; Oeschger, T. R.; Monteblano, M. M. *Tetrahedron Lett.* **1994**, *35*, 7751−7754.

(17) Ritter, H.; Drake, L. *Ind. Eng. Anal. Educ.* **1945**, *17*, 782−786.

S0002-7863(97)03449-5 CCC: $15.00
Published on Web 04/23/1998

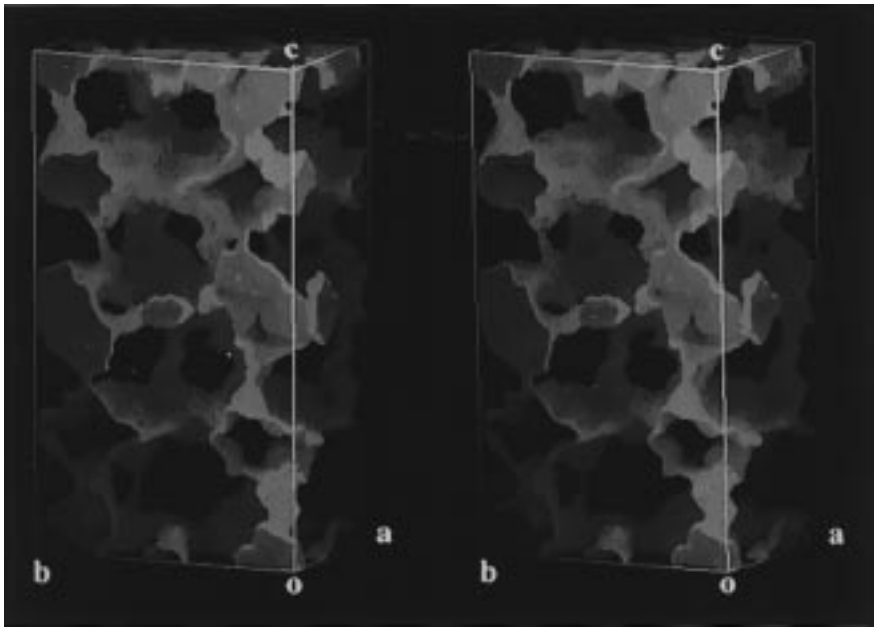

Figure 1. Stereo image of one unit cell of the crystal lattice of *C. rugosa* lipase (open form) crystals calculated from coordinates of the reported structure,[34] deposited in the Brookhaven Protein Data Bank.[35] In this picture, the enzyme molecules, which constitute the lattice, have been removed, and only the surface of the solvent channels has been contoured, with the solvent side of the channels in orange and the "protein-side" in violet. Channels are seen to traverse the crystalline unit cell (and, hence, the crystalline macroscopic sorbent particles) predominantly in the direction of the crystallographic *a* axis, with significant cross-channels in the crystallographic *b* axis direction. Far narrower channels can be seen along the *c* axis.

cury is forced to fill the pores under high pressure, as well as an adsorption of the vapor of an inert solvent (BET),[18] where the adsorption of nitrogen in the cavities of porous materials is measured at cryogenic temperatures. Both of these methods are intrinsically inappropriate for protein crystals, and have produced inconsistent and physically misleading results in our hands.[19] MIP is a particularly harsh and destructive procedure and often gives ambiguous results when significant sample compression occurs. In turn, the cryogenic temperature of the BET procedure is likely to solidify the largely aqueous solvent pores that constitute protein crystals,[5] resulting in artificially low measurements of apparent surface area. Indeed, the modern practice of cryogenic X-ray data collection is dependent on the deliberate vitrification of the crystallographic solvent channels to retard the damage to crystallographic order that follows irradiation.[20]

In order to characterize fully hydrated CLPC materials, therefore, we have opted to apply the method of macromolecular porosimetry[21] (see the Experimental Section). This technique allows one to estimate the apparent pore sizes and pore size distribution in solid and soft hydrated porous sorbents directly from size exclusion chromatography (SEC) experiments. The method has been successfully applied to silicas,[22] porous glasses, spherical alumina,[21] and gel filtration media.[22] SEC experiments with polyethylene glycol (PEG) standards were used to determine the porosity and pore volume of CLPC. To this end standard chromatography columns were packed with an aqueous slurry of CLEC formulations of thermolysin, lipases from *Candida rugosa* and *Pseudomonas cepacia*, and CLPC formulations of bovine and human serum albumins (BSA and HSA), using a slurry packing machine (Alltech) under a packing pressure of 1500−7000 psi. The porosity and average pore size for the different CLPC materials are presented in Table 1 together with literature data for inoganic zeolites.

As shown in Table 1, the experimental data on the porosity of CLPC are in good agreement with theoretical estimates of solvent content that are based on available crystallographic information for thermolysin and lipases (see also Figure 2). Protein crystals offer a wide variety of porous materials with a broad porosity range of 0.5−0.8, pore volumes of 0.9−3.6 mL/g, and pore surface areas of 800−2000 m^2/g (Table 1). In contrast, the corresponding numbers for zeolites[23] are 0.3−0.5, 0.2−0.4 mL/g, and 500−2000 m^2/g, respectively.

Pore size calculations based on a cylindrical pore model give narrow and symmetrical pore size distribution for all the CLPCs studied, with a calculated range of pore diameters that differ by less than 10% from the average (Table 1). One should keep in mind, however, that the channels within protein crystals have quite complicated structure which can hardly be described by a simple cylindrical model. Indeed, as a stereo image of the crystalline lattice of *C. rugosa* lipase suggests, a net of channels with narrow connecting necks are seen to traverse a crystal unit cell (Figure 1). Thus, it is not surprising that apparent pore sizes calculated from experimental SEC data are systematically larger than pore apertures measured from crystallographic data (Figure 2B,D). This difference can be rationalized by the inability of a simple geometric model to describe the complex structure of these materials and is not necessarily due to the experimental technique used, since other methods widely used in material science, such as BET and MIP, also rely on simple geometrical models for the calculation of pore sizes.

Protein crystals represent a distinct and unique class of molecular sieves, with a pore size range of 20 Å to more than

(18) Brunner, S.; Emmett, P. H.; Teller, E. *J. Am. Chem. Soc.* **1938**, *60*, 309−319.

(19) Both procedures were compared for thermolysin−CLEC. They gave inconsistent results, with pore size ranging from 306 Å (BET) to 500−600 Å (MIP), which are many-fold higher than that derived from X-ray crystallographic data (Table 1).

(20) Rodgers, D. W. In *Methods of Enzymology*; Carter, C. W., Jr., Sweet, R. M., Eds.; Academic Press: New York, 1997; Vol. 276, pp 183−217.

(21) Vilenchik, L. Z.; Asrar, J.; Ayotte, R. C.; Ternoroutsky, L.; Hardiman, C. J. *J. Chromatogr.* **1993**, *648*, 9−17.

(22) Hagel, L.; Ostberg, M.; Andersson, T. *J. Chromatogr.* **1996**, *743*, 33−42.

(23) Garces, J. M. *Adv. Mater.* **1996**, *8*, 434−437.

Table 1. Characteristics of CLPC and Other Sorbents

CLPC[a]/sorbent	particle shape and size[b]	porosity, $\epsilon_p = V_p/V_s$	solvent fraction	pore volume, mL/g of sorbent	pore surface area, m^2/g	apparent pore diameter, Å	aperture size, Å
thermolysin	rods; 7 μm	0.51	0.497	0.9	800	$46 + 2$[c]	25[d]
C. rugosa lipase	plates; 40 × 40 μm	0.50	0.494	0.9	900	38 ± 4[c]	15×25[d]
P. cepacia lipase	plates; 20 × 50 μm	0.80	0.738	3.6	1800	82 ± 10[c]	NA[e]
HSA	rods; 7 μm	0.65	NA[d]	2.0	1500	54 ± 8[c]	NA[e]
BSA	rods; 10 μm	0.67	NA[d]	1.8	1900	38 ± 3[c]	NA[e]
zeolites	spheres; varies	0.3−0.5[f]		0.2−0.4[g]	500−2000[e]	2−10[h]	

[a] For CLPCs the porosity, ϵ_p, was measured in the SEC experiments (see the text). The crystalline solvent fraction was calculated as described by Matthews.[5] The pore volume per gram of sorbent (V_p/g) for CLECs was calculated using the expression $V_p/m = (1/\rho)\,\epsilon_p/(1 - \epsilon_p)$, where m is the CLPC mass inside the column, ϵ_p is porosity, and ρ is the protein density; the latter is close to 1.1 (g/mL) for glutaraldehyde cross-linked protein crystals.[41] The pore surface area was calculated using a cylindrical pore model, where the surface area $S_p = 2\pi rl$ and the pore volume is $V_p = \pi r^2 l$. Consequently, $S_p = 2V_p/r$, where l is the cylinder length. [b] The average size of CLPC particles is from photomicrograph measurements. [c] Calculated by methods of macromolecular porosimetry (see the Experimental Section). [d] Calculated from computer-generated images in Figure 2B,D. [e] Crystallographic data are not available. [f] Data are taken from ref 23. [g] Calculated according to a cylindrical pore model, $V_p = Sr/2$. [h] See ref 42.

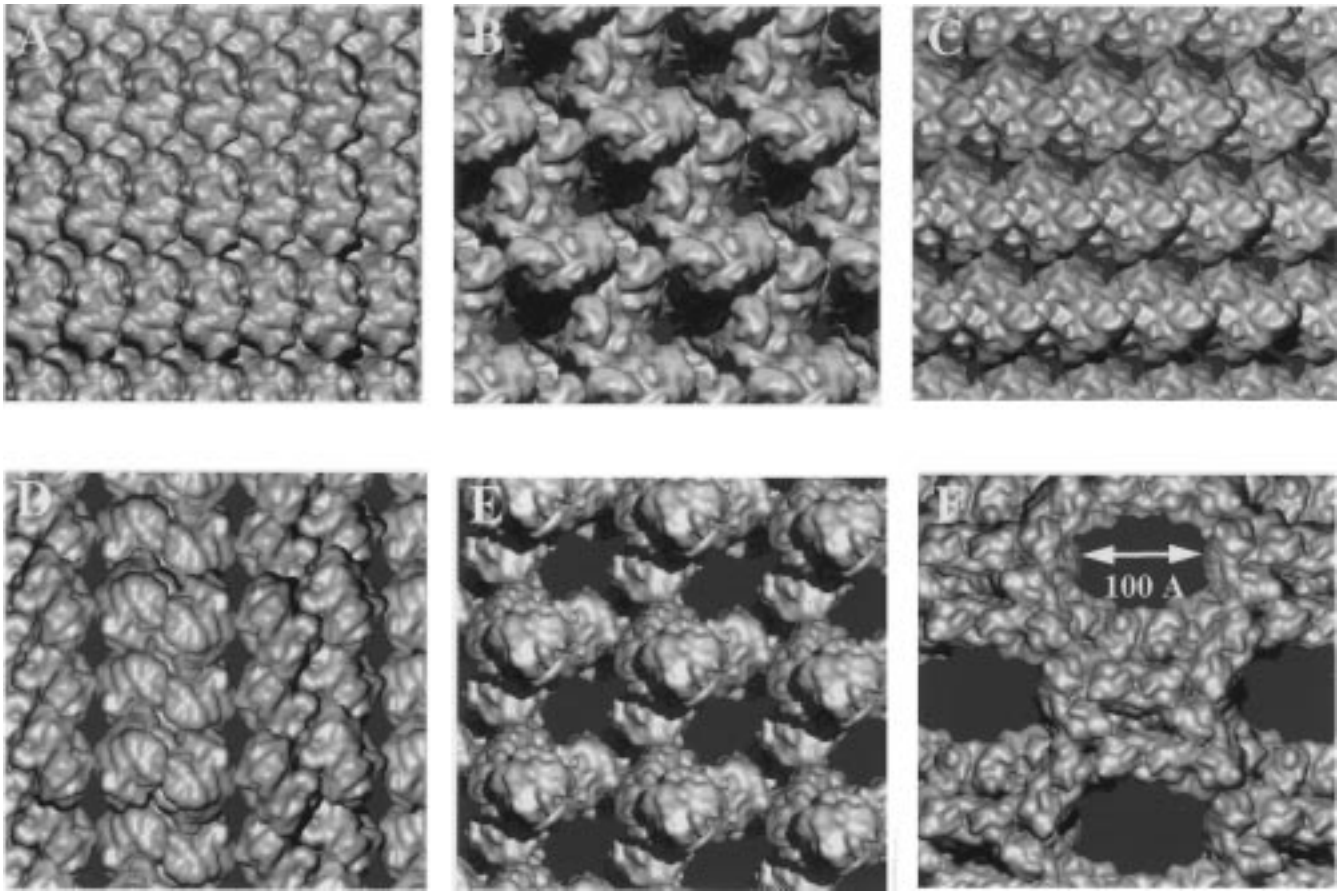

Figure 2. Computer-generated images of six different enzyme crystal lattices. The surface representation for each of these was computed from electron density that was calculated using coordinates from the corresponding solved crystal structures deposited in the Brookhaven Protein Data Bank.[35] Contouring isovalues were chosen to yield a surface whose enclosed volume approximates that of the molecule. The width and linearity of the solvent channels (shown in blue) depends in large part on the way the molecules pack in a particular space group. For example, crystals of human superoxide dismutase (F) have wide solvent channels that directly traverse the crystal, whereas molecules of superoxide dismutase from *Xenopus laevis* form crystals with tighter packing and solvent channels that are relatively narrow and convoluted (A). The corresponding coordinate file name and reference are given for each entry: (A) 1XSO,[36] superoxide dismutase *(X. laevis)*; (B) 8TLN,[37] thermolysin *(Bacillus thermoproteolyticus rokko)*; (C) 1PNL,[38] penicillin acylase *(Escherichia coli)*; (D) 1CRL,[34] lipase *(C. rugosa)*; (E) 1WHS,[39] carboxypeptidase W (wheat germ); (F) 1SOS,[40] superoxide dismutase (human recombinant). All structures are done on the same scale. The bar corresponding to 100 Å establishes the absolute scale of the figure.

100 Å in diameter (see, e.g., Figure 2), which is much larger than the pores in zeolites (Table 1). Equally important is the range of pore sizes that one can attain with a given protein material. In many instances, the same functional protein derived from different sources can yield dramatically different pore sizes, as with the *Xenopus* and human superoxide dismutases in Figure 2A,F, respectively. Even the identical protein can demonstrate crystalline polymorphism (in response to the detailed crystallization conditions employed), leading to different pore sizes and structure. Carter *et al.*,[24] for example, in their tabulation of the solvent content of various human and non-human serum albumin crystal forms, have demonstrated a broad range of solvent content (from a low of 33% to a high of 78%) across seven human serum albumin crystal forms. It should be noted

(24) Carter, D. C.; Chang, B.; Ho, J. X.; Keeling, K.; Krishnasami, Z. *Eur. J. Biochem.* **1994**, *226*, 1049−1052.

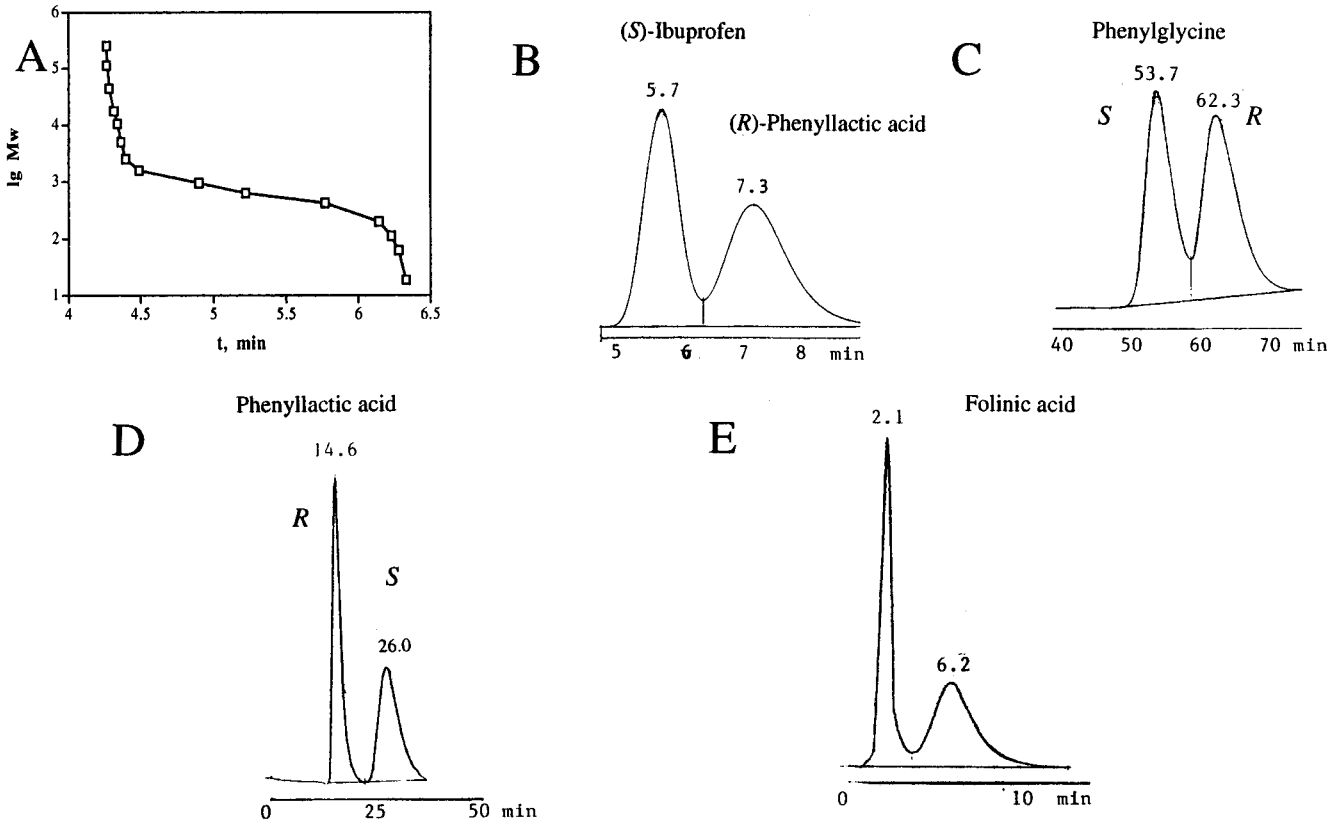

Figure 3. Thermolysin−CLEC was packed in a standard stainless steel column (25 cm × 4.6 mm). HPLC analyses were conducted with a Hewlett-Packard LC-1050 using a differential refractometer as detector for PEG solutions and UV detector (λ = 218 nm) for all other separations. (A) Mobile phase: Tris buffer, 10 mM, pH 7.4. Flow rate 0.5 mL/min; PEG samples with average molecular weight from 64 to 245 000; PEG concentration 3 mg/mL; injection volume 20 μL. A water molecule (MW 18) is also placed on the graph. Each PEG sample was injected separately, and the retention times of the chromatographic peak maxima were plotted against the MW of each sample. (B) Mobile phase: Tris buffer 10 mM, pH 8.15. Flow rate 0.5 mL/min; sample concentration 0.2 mg/mL; injection volume 20 μL; $k_1 = 1.1$, $k_2 = 1.7$, $\alpha = 1.6$ (C) Mobile phase: Tris buffer, 10 mM, pH 7.5. Flow rate 0.2 mL/min; sample concentration 2 mg/mL; injection volume 10 μL; $k_1 = 3.3$, $k_2 = 4.0$, $\alpha = 1.2$. (D) Mobile phase and flow rate: same as in C. Sample concentration 5 mg/mL; injection volume 1.5 μL; $k_1 = 2.5$, $k_2 = 5.2$, $\alpha = 2.1$. (E) The mixture of HSA−CLPC (16%) and silica (84% was packed in a 50 × 4 mm column. Mobile phase: sodium phosphate 100 mM, pH 6.9. Flow rate 0.7 mL/min; sample concentration 1.2 mg/mL; injection volume 0.5 μL; $k_1 = 4.9$, $k_2 = 16.3$, $\alpha = 3.3$. Neither the separation conditions nor the particle size and shape of the sorbent were optimized.

that chemical cross-linking, while making protein crystals more stable,[25] generally induces little change in pore structure, as demonstrated by X-ray diffraction patterns, indicating the close similarity of native and cross-linked forms.[26,27]

Since the pore size (Figure 2) and porosity (Table 1) of CLPC can vary with the nature of the protein, its source, and its crystallization conditions, one can create a variety of new microporous materials. Further, since proteins are weak ion exchangers with isoelectric points from 2 to 12, one can easily manipulate the binding of small molecules by changing the pH and buffer content of the eluent.

Of the many possible uses one may consider for CLPC, the most direct and immediate application is in the area of chromatography (Figure 3). Thermolysin−CLECs (rodlike particles, 7 μm in length)[13] provide good separation capability through at least three different mechanisms: size exclusion (Figure 3A), adsorption (Figure 3B), and chirality (Figure 3C,D). The ability of CLPCs to separate molecules by size may stem from the porous structure of the crystals (Figures 1 and 2). Indeed, as Figure 3A indicates, large PEG molecules do not seem to be able to penetrate the pores of thermolysin−CLECs. Very small molecules (MW < 100) enter the stationary phase and move equally slow without good separation. The PEG molecules between those two extremes (MW 100−10000) enter the pores of the stationary phase to varying extent according to their MW. The fact that PEG retention time does not depend on either the concentration of PEG or the elution rate (data not shown) suggests that PEG molecules do not have adsorption interaction with the stationary phase and are separated by the classical size exclusion mechanism.

In contrast, separation of small molecules by their chemical structure and chirality can be attributed to the protein nature of the stationary phase. For example, HSA−CLPC gave good resolution of two enantiomers of folinic acid (Figure 3e). When the cross-linked precipitate of HSA was used in place of HSA−CLPC, however, no resolution of folinic acid occurred. Moreover, in sharp contrast to HSA−CLPC (Table 1) the precipitate had extremely low porosity and was incapable of separating PEG. These results suggest that CLPCs effect separations by a unique mechanism involving the penetration of molecules into the ordered porous interiors of individual protein crystals. Indeed, if one approximates the rodlike crystals of HSA by a cylinder with a length (l) of 7 μm and radius (r) of 1 μm (Table 1), one can calculate that the surface area of such a particle (S) per gram of its mass equals 2.1 m^2/g.[28] At the same time the pore surface area of such a particle is 1500 m^2/g (Table 1).

(25) Quiocho, F. A.; Richards, F. M. *Biochemistry* **1966**, *5*, 4062−4076.
(26) Kasvinsky, P.; Madsen, N. *J. Biol. Chem.* **1976**, *251*, 6852−6859.
(27) Yonath, A.; Sielecki, A.; Moult, J.; Podjarny, A.; Traub, W. *Biochemistry* **1977**, *16*, 1413−1417.

Thus, one can conclude that the outer surface of a particle represents significantly less that 1% of the pore surface. Our preliminary experiments with HSA−CLPC indicate that even without further optimization the full separation of enantiomers of folinic acid can be achieved with loading of 2−3 mg per gram of CLPC. On the basis of the assumption that the molar binding ratio of folinic acid (MW 511) to HSA (MW 66 000) is 1/1, this loading level translates to greater than 30% of the theoretical binding capacity of the CLPC.[29] Thus, the crystallinity of the CLPC appears to have a critical role for both SEC and chiral separations.

It should be emphasized that the compounds separated in this study (PEG, ibuprofen, (*R*,*S*)-phenyllactic acid, and (*R*,*S*)-phenylglycine; Figure 3) are not substrates for thermolysin, so that no enzyme-catalyzed reaction has occurred in the course of the separation. While the ability of immobilized proteins, such as human serum albumin, α_1-acid glycoprotein, and cellobiohydrolase, to separate enantiomers is well known,[30] the chiral resolution properties of thermolysin have never been reported. Both thermolysin−CLEC and HSA−CLPC were found to be fairly stable both in column packing (a packing pressure of 1500 psi was applied) and in the chromatography experiments themselves (more than 500 injections were performed without loss of separation efficiency). Further, the repeated changes of eluent from water to 50% acetonitrile did not influence the efficiency of chiral separations, thus indicating high stability of the stationary phase.

The bioorganic zeolites we have formulated here have several features in common with their inorganic counterparts. Both are crystalline microporous materials with a uniform pore size distribution that is fixed by arrangement of their unit cells. While zeolites are much more stable thermally, protein crystals may offer more control over pore size, porosity, and chemical properties of the pore surface.

In addition to separations cross-linked protein crystals may find significant new applications as sorbents, as catalysts, and in sensing devices. The combination of the variety of available proteins (several thousands are known) with recent advances in protein bulk crystallization and cross-linking[9] opens almost unlimited opportunities to create and produce cost-efficient, well-defined microporous materials.

Experimental Section

Materials. CLEC formulations of thermolysin and lipases from *C. rugosa* and *P. cepacia* are commercial products of Altus Biologics. Crystallization of BSA and HSA was accomplished by adding an ammonium sulfate solution (767 mg/mL) to BSA (250 mg/mL) and HSA (120 mg/mL) that was dissolved in 100 mM phosphate buffer (pH 5.3) at 4 °C. CLPCs were obtained by cross-linking of these crystals with glutaraldehyde according to the published procedure.[7] The standard chromatography columns (50 × 4.6 mm, 100 × 4.6 mm, and 250 × 4.6 mm) were packed with about 0.5, 1, and 2.5 g each of an aqueous slurry of CLEC formulations.

Porosity Measurements. The porosity of materials, ϵ_p, is equal to the volume of the porous space V_p divided by the total sorbent volume V_s ($\epsilon_p = V_p/V_s$). PEG retention time does not depend on either the concentration of PEG or the elusion rate (data not shown). These results suggest that PEGs do not have adsorption interaction with the stationary phase and can be used as specific probes that penetrate the crystal pores in accordance with the size of the molecules.[31] It is assumed that the smallest PEG molecules (MW 62, radius of gyration 3.0 Å) penetrate all the channels within and between the crystals (pore size at least 20 Å). The size of the PEG samples was calculated according to the Flory−Fox equation with the Ptitzyn−Eisner modification for excluded volume.[31] The product of the volumetric flow rate U and the retention time, t_{62}, for PEG molecules with MW 62, is equal then to the sum of the volume of porous space V_p and the volume of channels V_o between the sorbent particles inside the packed column ($V_p + V_o = t_{62} \times U$). On the other hand, the largest PEG sample used in the study (MW 500 000, radius of gyration 360 Å, and corresponding retention time $t_{500\ K}$) can only penetrate the channels between the sorbent particles, and thus $V_o = t_{500\ K} \times U$. Therefore, in order to measure the porosity from SEC data one simply needs to find $V_p = (t_{62} - t_{500\ K})/U$ and divide it by the volume of the sorbent inside the column, V_s, which is equal to the difference between the column volume V_c and the mobile phase channels' volume V_o ($V_s = V_c - V_o$).

Pore Size Distribution. In the method of macromolecular porosimetry, which is described in detail in ref 21 and critically analyzed and reviewed in ref 22, solubilized macromolecules such as PEG are used as specific probes. Reliable expressions for the distribution coefficient (K_d) between porous space and the free volume are known[32,33] for different pore shapes as a function of the ratio of the radius of the macromolecule (R) and the radius of the sorbent pore (r). A comparison of theoretical K_d values with experimental values obtained from the SEC data allows one to calculate the sorbent's pore size distribution.

Acknowledgment. We thank Chandrika Govardhan and Nazer Khalaf for their help and fruitful discussions and the National Science Foundation (Grant DMI-9660460) for its support.

JA973449+

(28) The surface area of a cylinder (S) equals $2\pi rl + 2\pi r^2$ and the mass of such a particle will be $m = \pi r^2 l\rho$, where l is the cylinder length, r is its radius, and ρ is the crystal density. Consequently, $S/m = 2/\rho(1/r + 1/l)$. In the case of HSA crystals $l = 7\ \mu$m, $r = 1\ \mu$m, and ρ is close to 1.1 mg/cm^3 (Table 1). Thus, $S/m = 2.1$ m^2/g.

(29) The authors are grateful to Reviewer II for making this point.

(30) Hermansson, J. Proceedings of the Chiral Europe 95 Conference, September 1995, pp 95−114.

(31) 1. Belenkii, B. G.; Vilenchik, L. Z. *Modern Liquid Chromatography of Macromolecules*; Elsevier: New York, 1984; pp 101−105.

(32) Giddings, J. C.; Cucera, E.; Russel, C.; Myers, M. *J. Phys. Chem.* **1968**, *72*, 4397−4408.

(33) Casassa, E. *J. Polym. Sci.* **1967**, *B5*, 773−778.

(34) Groschulski, P.; Li, Y.; Schrag, J. D.; Bouthillier, F.; Smith, P.; Harrison, D.; Rubin, B.; Cygler, M. *J. Biol. Chem.* **1993**, *268*, 12843−12847.

(35) Bernstein, F. C.; Koetzle, T. F.; Williams, G. J. B.; Meyer, E. F., Jr.; Brice, M. D.; Rodgers, J. R.; Kennard, O.; Shimanouchi, T.; Tasumi, M. *J. Mol. Biol.* **1977**, *112*, 535−542.

(36) Holland, D. R.; Rronrud, D. E.; Pleyk, H. W.; Flaherty, M.; Stark, W.; Jansonius, J. N.; McKay, D. B.; Matthews, B. M. *Biochemistry* **1992**, *31*, 11310.

(37) Holland, D. R.; Tronrud, D. E.; Pleyk, H. W.; Flaherty, M.; Stark. W.; Jansonius, J. N.; McCay, D. B.; Matthews, B. W. *Biochemistry* **1992**, *31*, 11310−11316.

(38) Duggleby, H. J.; Tolley, S. P.; Hill, C. P.; Dodson, E. J.; Dodson, G.; Moody, P. C. E. *Nature* **1995**, *373*, 264−268.

(39) Liao, D.-I.; Remington, S. J. *J. Biol. Chem.* **1990**, *265*, 6528−6531.

(40) Parce, H. E.; Hallewell, R. A.; Tainer, J. A. *Proc. Natl. Acad. Sci. U.S.A.* **1992**, *89*, 6109.

(41) Matthews, B. W. *Methods Enzymol.* **1985**, *114*, 176−187.

(42) Davis, M. E.; Katz, A.; Ahmad, W. R. *Chem. Mater.* **1996**, *8*, 1820−1839.